



UNIVERSITY OF LEEDS

This is a repository copy of *Establishment of a preconditioning regime for air permeability and sorptivity of alkali-activated slag concrete*.

White Rose Research Online URL for this paper:
<http://eprints.whiterose.ac.uk/111913/>

Version: Accepted Version

Article:

Yang, K, Yang, C, Magee, B et al. (2 more authors) (2016) Establishment of a preconditioning regime for air permeability and sorptivity of alkali-activated slag concrete. *Cement and Concrete Composites*, 73. pp. 19-28. ISSN 0958-9465

<https://doi.org/10.1016/j.cemconcomp.2016.06.019>

Crown Copyright © 2016 Published by Elsevier Ltd. This manuscript version is made available under the CC-BY-NC-ND 4.0 license
<http://creativecommons.org/licenses/by-nc-nd/4.0/>

Reuse

Unless indicated otherwise, fulltext items are protected by copyright with all rights reserved. The copyright exception in section 29 of the Copyright, Designs and Patents Act 1988 allows the making of a single copy solely for the purpose of non-commercial research or private study within the limits of fair dealing. The publisher or other rights-holder may allow further reproduction and re-use of this version - refer to the White Rose Research Online record for this item. Where records identify the publisher as the copyright holder, users can verify any specific terms of use on the publisher's website.

Takedown

If you consider content in White Rose Research Online to be in breach of UK law, please notify us by emailing eprints@whiterose.ac.uk including the URL of the record and the reason for the withdrawal request.



eprints@whiterose.ac.uk
<https://eprints.whiterose.ac.uk/>

Establishment of a preconditioning regime for air permeability and sorptivity of alkali-activated slag concrete

Kai Yang^{a,b,c*}, Changhui Yang^a, Bryan Magee^d, Sreejith Nanukuttan^b, Jianxiong Ye^a

a: College of Materials Science and Engineering, Chongqing University, Chongqing, China

b: School of Planning, Architecture and Civil Engineering, Queen's University Belfast, Belfast, UK

c: School of Civil Engineering, University of Leeds, UK

d: School of the Built Environment, Ulster University, Newtownabbey, UK

Abstract

This study reports an experimental investigation designed to assess the influence of near-surface moisture contents on permeation properties of alkali-activated slag concrete (AASC). Five different drying periods (5, 10, 15, 20 and 25 days) and three AASC and normal concretes with compressive strength grades ranging from C30 to C60 were considered. Assessment of moisture distribution was achieved using 100 mm diameter cores with drilled cavities. Results indicate that air permeability of AASC is very sensitive to the moisture content and its spatial distribution, especially at relative humidity above 65%. To control the influence of moisture on permeation testing, the recommendation of this paper is that AASC specimens should be dried in controlled conditions at 40 °C for 10 days prior to testing. It was also concluded from this study that AASC tends to perform less well, in terms of air permeability and sorptivity, than normal concrete for a given strength grade. This conclusion reinforces the need to further examine AASC properties prior to its widespread practical use.

Keywords: alkali-activated slag concrete, relative humidity, sorptivity, porosity, air permeability

1. Introduction

Impacts of climate change on society are evident from the recent events and concentration of CO₂ in the atmosphere presents a major factor closely linked with global temperature fluctuations [1]. With the cement industry representing around 5% of global CO₂ emissions [2], development of innovative, low CO₂-impact binding materials is an area attracting intense research interest at present.

One possible alternative is alkali-activated slag, which is a clinker-free binder significantly differing from traditional Portland cement (PC) [3-5]. The production of 1 tone of alkali-activated slag emits around 0.18 tonnes of CO₂ to the environment, approximately 80% less than ordinary PC [2,4,5]. Encouragingly, previous research [5-9] confirms that alkali-activated slag concrete (AASC) offers a range of performance benefits, such as high mechanical strength at early stages of curing, excellent acid-resistant characteristics, good resistance to freeze-thaw cycles and resistance to elevated temperatures. As such, the production and performance of AASC have been a highly active area of academic and industrial research over the past decades. Despite this fact, however, the widespread commercial adoption of AASC has been limited to date owing to, in part, its relatively limited record of durability in service [4, 10].

To become established as a successful alternative to PC-based concrete, AASC must offer similar durability and long-term resistance levels to aggressive agents. To address this issue within a realistic experimental timeframe, developing an understanding of cover concrete permeation properties (including water absorption, permeability and diffusivity) directly impacting ingress rates of aggressive substances from the environment, is essential [11-13].

Prior to all permeation testing, initial conditions of samples must satisfy certain requirements as specified in classical theories [14, 15]. Drying is an unavoidable preconditioning procedure for gas permeability [11, 16], gas adsorption [17], gas diffusion [18] and water absorption [19, 20]. However, despite the existence of numerous drying methods for PC samples [21-23], no drying methods have

specifically been developed for AASC to date. While the effect of different drying techniques on the microstructure of conventional PC samples is well studied [21, 22, 24, 25], proposed techniques are likely not be suitable for drying AASC samples due to inherent microstructural and gel chemistry differences. As Collins and Sanjayan [26] have pointed out, AASC samples are more sensitive to moisture loss than PC-based materials and may undergo a continuous sequence of irreversible decomposition reactions during drying. As such, AASC physical and chemical properties might be significantly changed, meaning that pre-conditioning procedures may impact test results and give potentially misleading conclusions regarding long-term in-service performance [27, 28]. Meanwhile, the correct interpretation of permeation test results requires determination of internal moisture content and its distribution [11, 29]. This is a further area where in-depth research is lacking for AASC. It is, therefore, not surprising that no specific moisture requirements have been established for evaluating permeation properties of AASC.

Against this background, the main aim of this work is to propose a preconditioning regime suitable for obtaining reliable data when measuring AASC permeation properties. To achieve this, a research programme was undertaken to establish effects of various preconditioning regimes and moisture contents on key properties including relative humidity, air permeability, sorptivity and porosity.

2. Experimental programme

Three strength classes (C30, C45 and C60) of both normal concrete (NC) and AASCs were considered to represent common structural applications and enable direct performance comparisons. In terms of moisture conditioning, samples were exposed to oven drying at 40 °C for a range of periods (5, 10, 15, 20 and 25 days) and then assessed for both moisture movement during the preconditioning process and subsequent permeation properties (including air permeability and sorptivity measurements). General properties of the concretes were also assessed, including slump, air content and 28-day compressive strength. The overall scope of the test program is given in **Table 1**.

In terms of the drying regime used in this study, comparison of drying techniques used for normal concrete (NC) confirms oven drying as the most commonly due to its simplicity and rapidity [21, 23]. While it is known [11, 16, 17] that high drying temperature can induce microstructural changes of cementitious materials due to physical and chemical reactions, this is particularly true for AASC. Indeed, several studies have indicated that oven drying as low as 60 °C can cause significant pore structure alteration in alkali-activated slag paste samples [10, 27]. From previous research, a drying temperature of 40 °C has been reported as appropriate for minimising cementitious microstructural alteration and capable of determining free moisture contents of NC and AASC samples [11, 27, 30] and removing moisture effects on permeation results of a range of concrete types [11, 29]. As such, the temperature of 40 °C was chosen as the pre-conditioning drying temperature for AASC in this study.

2.1 Alkali-activated slag concrete mix proportion and raw materials

Based on previous related research [31-33], the mix proportions of the concrete tested in this investigation are shown in **Table 2**. Granulated blast furnace slag (GBFS) supplied by Chongqing Iron and Steel Group and Portland cement (PC) conforming to GB-175 [34] were used throughout. The specific area of PC used in this study is 335 m²/Kg, 430 m²/Kg for GBFS. The chemical compositions of both PC and GBFS are given in **Table 3**.

The activator for AASC was a mixture of a liquid sodium silicate solution with a pre-specified modulus of MS=1.2 (defined as the mass ratio of SiO₂ to Na₂O). It was prepared by mixing a NaOH solution and liquid water glass (Na₂O: 29.03%, SiO₂: 12.07% by mass) in a pre-calculated ratio. The Na₂O dosage was kept constant for preparing AASC, 5% of the GBFS content.

The fine aggregate used was medium graded natural sand (fineness modulus: 2.60) and the coarse aggregate was 10 and 20 mm crushed basalt in equal proportions, conforming to GB/T-14684 [35] and GB/T-14685 [36], respectively. Aggregate moisture content was controlled by drying in an oven at

105±5°C for 24 hours followed by cooling in an environment controlled room (20±1°C, 55±10%) for one day before casting concrete.

2.2 Specimen preparation

For each concrete mix, constituent materials were batched by mass and mixed according to BS 1881: part 125: 1986 [37]. All fresh concrete was initially assessed for consistence (slump test) and air content [38]. Two 300×250×150 mm slabs and six 100 mm cubes were subsequently manufactured for each mix to facilitate permeation studies and compressive strength testing. Full compaction was ensured for all specimens using both vibrating table (cubes) and an internal flexible shaft vibrator (slabs) and was considered to be achieved when no air bubbles appeared on the concrete surface. After compaction, all specimens were covered with a polythene sheet, de-moulded the following day and placed in a curing room (temperature: 20±2°C, relative humidity: 95±5%). Cube specimens were removed at the age of 28 days and tested for compressive strength.

Slump, air content and compressive strength results are reported in **Table 2**. It indicates that corresponding AASC and NC mixes exhibited similar properties. For the AASC mixes, ranges of slump, air content and strength values recorded were 145-200 mm, 1.6-2.1 % and 34.5-66.5 MPa respectively. Corresponding ranges for the NC were 165-195 mm, 1.5-1.8% and 37.0-69.5 MPa. The conventional properties of AASC and NC are not discussed in detail, as attention will be confined to assess the moisture loss process and their influence on permeation properties of AASC and NC.

After 56 days, six 100 mm diameter cores were extracted from the slab specimens for each concrete and saturated by incremental immersion for 10 days. Incremental immersion involved exposure of one-half of the specimen to water initially to allow both water absorption and air removal. After 4 days, a further quarter of the depth was immersed before complete immersion after another 2 days. The whole process is shown in **Figure 1**, which allowed the specimens to be saturated by capillary action without trapping air [20]. At the completion of the saturation process, the saturated mass (M_0) and the dimensions (radius, r and length, l) were measured. The six cores for each mix were then placed in a

drying cabinet (temperature: 40 °C; relative humidity: 35 %) and were divided into two groups as follows:

- 1) Three cores were used to study the relationship between air permeability and moisture condition. After five different drying periods (5, 10, 15, 20 and 25 days), the three cores for each mix were removed from the oven, wrapped in a polythene sheet and cooled to room temperature (around 20°C, 55% RH) for 1 day. Air permeability and relative humidity measurements were then carried out and, the specimens placed in the drying cabinet. After undertaking the last set of air permeability and relative humidity tests, water absorption testing was carried out in accordance with BS-EN: 13057 to determine sorptivity values [39].
- 2) The other three cores for each concrete mix were used to assess capillary and gel porosity. To estimate capillary porosity, the cores were placed in the drying cabinet at 40 °C until constant mass (M_{40C}) was achieved. To assess gel porosity, the cores were then placed in an oven at 105 °C to reach the mass equilibrium state (M_{105C}). These procedures were developed based on the previous studies [11,27,29,30].

2.3 Test methods

2.3.1 Relative humidity on the surface and in the 20mm drilled hole

Relative humidity (RH) provides direct information about the content and distribution of moisture in the concrete sample and is considered a useful parameter in checking the reliability of an air permeability measurements; particularly when distinguishing between pore structure and moisture affects[14,16,20,21]. In this study, RH measurements were carried out on sample surfaces and within drilled 20 mm deep holes using an RH probe, which is shown in **Figure 2**. Prior to measurements, the sensor was calibrated using a saturated salt solution with a known RH.

After measurements were taken, the drilled holes were sealed with rubber plugs fitted with silicone to ensure that the reading in the cavity was not affected by ambient conditions. Both RH and temperature

was recorded for each measurement after stabilisation was reached; a process generally taking around 40 mins to achieve. Two replicates were performed for each test set (one measurement in each of the test cores), the mean value of which was reported.

2.3.2 Water absorption test

The sorptivity of concrete was determined according to the standard procedure provided in BS-EN: 13057, 2002 [39]. For each concrete, a 100 mm diameter core dried in the oven at 40 °C for 25 days was placed in contact with water in a shallow tray. Water was absorbed through the bottom surface and the mass gain of the specimen was measured every minute over a period of 16 minutes. To compute the value of sorptivity, the data points were fitted using linear regression in the form of Equation (1):

$$i = A + St^{0.5} \quad (1)$$

where i is the volume of water absorbed per unit area (mm^3/mm^2); S is a material constant called the sorptivity ($\text{mm}/\text{min}^{0.5}$); A is a constant (mm) and t is the time elapsed (min). The mean value of three measurements was reported along with the average error.

2.3.3 Air permeability test

Figure 3 shows the surface mounted air permeability test instrument used in this study to assess both AASC and NC, further details of which are reported in the literature [29]. The test area considered was the inner 50 mm circle of the 100 mm cylindrical specimen, isolated using a base ring. The instrument was manually pressurised by a syringe and when the pressure in the test chamber reached 0.5 bar, the test commenced automatically. The pressure inside the test chamber then decreased due to air escaping through the pores in each specimen. The rate of pressure decay was monitored every minute for 20 minutes and used to compute the air permeability index, API (unit: $\ln(\text{bar})/\text{min}$) using the following equation:

$$\text{API} = \frac{\ln \frac{P_i}{P_t}}{t_i - t_t} \quad (2)$$

where t is the time (s); P_i and P_t (N/m^2) are the pressures in the chamber at the start and at any time, t , respectively. Three samples were tested for each concrete mix.

To assess the influence of moisture on the air permeability, the API is normalised based on the RH in the 20 mm hole, which is shown as follows:

$$API_N = \frac{API_{AD}}{API_{25d}} \quad (3)$$

where API_N is normalised data, API_{AD} is the API after drying for different periods, API_{25d} is the API after drying for 25 days. With no physical meaning, the values obtained in this way were only used to establish the relationship between air permeability and relative humidity.

2.3.4 Capillary porosity and gel porosity

Porosity was determined by the mass difference of water-saturated and dried samples at different temperatures. In general, capillary porosity refers to the pore space occupied by water held by capillary force, the removal of which does not need high energy [25]. Previous researches [11,29,30] show that this property was estimated by drying saturated samples and measuring the weight loss under 40-50 °C and this weight loss is taken as an estimate of porosity of the capillary system. According to this, the gel pores were determined by the moisture loss under 40 °C and 105 °C, as the capillary pores and gel pores are two main types in concrete.

Capillary and gel porosity was determined on the basis of the mass (or moisture) loss of a saturated specimen dried at 40°C and 105°C, respectively, till constant mass and using the following equations:

$$\text{Capillary porosity: } f_c = \frac{M_o - M_{40C}}{\rho_w \pi^2 l} \times 100\% \quad (4-1)$$

$$\text{Gel porosity: } f_G = \frac{M_{40C} - M_{105C}}{\rho_w \pi^2 l} \times 100\% \quad (4-2)$$

where M_0 is the mass of a saturated sample (kg); M_{40C} and M_{105C} are the mass of a sample after drying at 40 °C and 105 °C (kg); ρ_w is the density of water (kg/m^3); r is the radius of the sample (m); l is the length of the sample (m).

2.3.5 Microstructure analysis

Pore structure characteristics of NC and AASC were determined by mercury intrusion porosimetry (MIP) and Scanning Electron Microscope (SEM). The MIP instrument was capable of a minimum intruding pressure of 0.52 psi (26.89 mmHg), and a maximum of 33000 psi (227 MPa), while the contact angle assumed in this study was 130°. The corresponding range of pore diameters was between about 350 μm and 5 nm. The intruded volume could be read to an accuracy of 0.1 μm . The microstructure analysis was performed with TESCAN VEGA 3LMH. In this apparatus, an image is transformed into more than 20kv electrical pulses, each corresponding to a square of the image-picture point. The size of a photo depends on the magnification used.

The size of the specimens was about 3-4 grams for concrete, which was obtained after compressive strength tests. The preparation involved the gentle drying at 40°C until constant weight reaches.

3. Results and discussion

3.1 Moisture condition after drying

Figure 4 shows a summary of RH results for both NC and AASC specimens after different drying periods. As expected, moisture loss from all concrete is reflected by a general trend of decreasing RH values with increasing drying periods. For RH values at the surface of both AASC and NC at different strength grades considered, it is also clear from **Figures 4-a** and **-c** that no typical patterns exist, suggesting that the concrete type and compressive strength level have minimal impact on the surface humidity during drying. With respect to RH within the drilled 20 mm cavities (**Figures 4-b** and **-d**), RH values were consistently higher than surface measured values. This indicates that, for both NC and AASC specimens, moisture gradients were formed during the drying process and a moisture equilibrium state was not established.

Furthermore, the results of AASCs show three distinct features compared with NC during the drying process. Firstly, drying for 10 days at 40 °C caused a substantial RH drop at the 20mm cavity (from 80% to 60%) and further drying did not result in significant RH reductions. On the contrary, a more constant rate of reduction in RH readings for NC was observed. Secondly, no noticeable difference in RH within the 20 mm cavities was identified for the three AASCs considered, suggesting a minimal impact of compressive strength grade (or w/b) on 20 mm RH. For NC, a more noticeable difference in RH values with time existed between different mixes. This was most pronounced for the C30 mix, which consistently exhibited higher (on average 5%) RH levels than C45 and C60 mixes across the drying time intervals considered. Differences of C45 and C60 were less significant. Lastly, the RH results of AASC were consistently lower than NC during the drying process.

The above observations emphasise the influence of concrete type on the features of moisture loss in the drying process and are consistent with results obtained with related studies [10,11,21,30]. While few reports documenting the moisture loss characteristics of AASC are available presently, a comparison can perhaps be drawn to concretes containing large amounts of supplementary cementitious materials, in particular GBFS, given their similarity to AASCs in terms of hydration products and microstructure. Indeed, investigations of concretes comprising 50 % GBFS concluded that they tend to dry more rapidly than similar concrete made with plain Portland cement [29, 40]; a trend consistent with the results obtained from this study.

On the other hand, the rapid moisture loss noted for AASC in 1-10 days may be considered surprising, given that numerous reports have shown its pore structure tends to be very dense and impermeable [10, 28, 41]. An explanation for this may be the different role of water in AASC compared to NC. Water in AASC plays an important role in the kinetics of dissolution of ionic species and polymerisation processes. In the hardened state, it exists as absorbed water inside pores or as condensed hydroxyl groups on the surface of the calcium silicate hydrate (C-S-H) gel. It is believed that the water does not notably participate in the formation of the main product phases and does not form a strongly hydrated

binder phase similar to Portland cement. Therefore, water in AASC is reported to be easily removed from specimens [27, 42, 43].

Another feature noticeable from **Figure 4** is that for both AASC and NC, most readings became stable after drying for 25 days, varying from 40 to 60%.

Considering the variation of RH results, evaporable moisture in the AASC specimens dried out more quickly than for NC. After drying for 10 days, the RH values for AASCs were typically around 60 %, regardless of compressive strength grade. Consequently, the main conclusion drawn from this element of the study is that the required pre-conditioning period for AASC is a minimum of 10 days. This is considerably less than NC, which requires at least 20-day drying to achieve a similar moisture condition.

3.2 Porosity and sorptivity

Regarding the relationships of RH versus drying duration plotted in **Figure 4**, the controlling influence on the trends noted was capillary moisture loss, which occurred at the controlled drying environment of 40 °C considered. Not affecting the results in **Figure 4** was physically bonded or adsorbed moisture on gel surfaces, which is typically lost at temperature around 105 °C [14, 23, 27, 44]. In this element of the study, therefore, both capillary and the gel porosities were determined on the basis of the moisture of 40 °C and 105 °C respectively.

Influences of concrete type and compressive strength grade on capillary and gel porosity are shown in **Figure 5**, which for both AASC and NC shows increasing total porosity with decreasing compressive strength; an expected trend due to established relationships between w/b ratio and compressive strength [25, 45]. At all three strength grades considered, also clear from **Figure 5** is consistently higher total porosity for AASC (ranging from 10.13 to 13.12%) compared to NC (ranging from 8.77 to 12.79%). This is justifiable given the inherently high strength binder systems associated with AASC [6, 7, 9].

As such, for a given compressive strength grade a higher water/solid ratio was used for AASC, relative to NC (see **Table 2**), thereby resulting in higher levels of ultimate porosity.

Sorptivity is a key parameter when assessing concrete durability, particularly developing an understanding of water transport process under the unsaturated conditions [10, 18, 45-47]. As obtaining reliable values and interpreting test results correctly requires all evaporable moisture in the test sample to be removed initially, all water absorption testing in this study was carried out on specimens dried at 40 °C for 25 days. This time period was selected based on the results published in **Figure 4**, which showed stabilised values of moisture for both AASC and NC at this time. Resultant sorptivity values obtained are plotted in **Figure 6**.

Clearly for both AASC and NC, sorptivity values increased with decreasing compressive strength grade (or increasing w/b ratio). Also clear from **Figure 6** are markedly higher values of AASC sorptivity relative to NC for each strength grade considered. Sorptivity values for NC strength grades C30, C45 and C60 were 1.00, 0.72 and 0.47 mm/min^{0.5} respectively, while corresponding values for AASC were 3.14, 2.15 and 1.19 mm/min^{0.5}. As capillary porosity and moisture distribution are similar for both concrete types (as indicated in **Figure 4** and **5**), this observation cannot be solely explained by a higher w/b ratio for AASC.

This seems contrary to previous research [4, 44], which based on porosimetry and microstructural studies reported alkali-activated slag binder systems to comprise smaller pores with a higher surface area relative to cement binder systems with similar porosity. It should be highlighted that these investigations generally focussed on the gel porosity (and not capillary porosity) of paste samples. As the full complexity and characteristics of pore structures can only be captured through microscopic examination, volumes of materials analysed were small and observations perhaps not statistically representative of pore connectivity at a more macroscopic scale. Permeation properties, e.g. sorptivity, permeability, diffusivity, are more sensitive to capillary porosity and pore connectivity. Several studies

for AASC also show that the sorptivity of AASC is lower than that of NC, but performance comparisons made in these studies was not based on similar compressive strength grade and, more importantly, no relevant moisture conditions were reported [28, 46, 48, 49]. As such, relevant comparisons with results presented in this study cannot be directly made. As explained previously, evaporable moisture was removed from all specimens prior to testing under the similar moisture condition, higher sorptivity values for AASC were clearly seen in **Figure 6**. The observed trend may be due to the effect of connectivity in the emptied pores and it is likely that the capillary pore network of AASC is more connected or less tortuous than the pore networks developed in NC. To further prove this point, SEM and MIP were used to compare the microstructure characteristics of AASC and NC.

Figure 7 shows SEM results of AASC and NC. A relatively low magnification (500×) is large enough to include essential features of binder phase which is given in **Figure 7 a-1** (AASC C60), **a-3** (AASC C30), **b-1** (NC C60) and **b-3** (NC C30). For AASC, uniform hydration products are found and no crystal is seen, while fragments of several different crystals are present in NC and the surface of its hydration products is not smooth as AASC. Furthermore, the shape of pores in AASC is significantly different from that in NC for a given compressive strength grade. More specifically, despite of denser hydration products, AASC has shown cracking patterns and relatively more pores as illustrated in **Figure 7**, but within hydration products display little detectable pores. For NC, the pores appeared to be relatively few in number and generally performs like a hole. This feature can be shown in detail at higher magnification in **Figure 7 a-2** (AASC C60), **a-4** (AASC C30), **b-2** (NC C60) and **b-4** (NC C30). It can also be found in AASC samples that some visual pores are interconnected, whereas pores in NC samples seem isolated with each other.

Pore size distribution of AASC and NC was determined through MIP measurements. Data summarised in **Figure 8**, show the occurrence of pores in AASC and NC. Apparently, for a given compressive strength grade, the porosity of AASC is much higher than NC which is consistent with the results of capillary porosity shown in **Figure 5**. In addition, AASC has more fine pores than NC especially for

pores with diameter less than 50nm, but there are less coarse pores in AASC. This observation agrees well with previous results that have suggested that AASSC has a dense pore structure [4,8]. By means of a pattern recognition system, it is possible to characterise the threshold pore diameter estimated by measuring highest variation of pore volume. For AASC C60 and C30, the threshold pore diameter is approximately 80nm, meaning that the w/s ratio does not play an important role. For NC, however, the situation is significantly different, as the threshold value of C60 is around 10 nm and much lower than C30 (around 95nm). As such, there are more relatively single continuous pores occur in AASC. This allows rapid bypassing of the pores. As expected from the comparatively low w/b ratio used, the proportion of pores was limited. It suggests that water or air flow pathways in AASC might be self-organising into a network structure and the significant difference in water absorption behaviour between AASC and NC must be due to the occurrence of relatively large and continuous voids in AASC.

In this study, comparisons of sorptivity between AASC and NC were based on equivalent compressive strength grade under the moisture free condition and for a given compressive strength grade, AASC tends to have a higher water/solid ration, which naturally results in a higher permeation characteristic. In addition, the sorptivity reflect the near-surface properties, while most current studies focus on measuring the permeation properties of the whole sample [13,14,29]. The difference between the near-surface zone and core section may be another factor contributing the observed trend.

3.3 Air permeability after drying

An air permeability index (API) was determined for each NC and AASC mix using the surface mounted permeability test equipment as described previously. To evaluate the effect of drying durations on the results obtained, all specimens were initially dried in an oven at 40 °C for 5 different durations (5, 10, 15, 20 and 25 days).

The relationship between API and drying period are plotted in **Figure 9**, which clearly indicates generic effects of compressive strength (increasing strength resulting in decreasing API), concrete type (API higher for AASC than NC for each strength grade considered) and drying duration (generally increasing API values with increasing drying period). In terms of the latter effect for AASC, an increase in drying period from 5 to 10 days resulted in a significant rise of API (more than 200%), with increases beyond this time diminishing significantly in value (less than 5%). This trend suggests that for AASC, undertaking air permeability measurements after a minimum of 10 days initial drying at 40 °C is likely to minimise the risk of result being compromised by moisture effects. For NC, on the other hand, results obtained from this study compare favourably with previously published data [11, 40], indicating minimal effects of moisture on API beyond 20 days of initially drying at 40 °C [29, 50].

To further investigate the influence of moisture on air permeability of AASC and establish a moisture requirement for a reliable air permeability measurement, **Figure 10** provides the normalised air permeability for AASC and NC plotted against corresponding RH values measured in the 20 mm deep specimen cavities. It is clear that AASC and NC follow a similar trend. More specifically, at RH below 65%, the normalised air permeability of both AASC and NC are generally constant, suggesting that moisture effect has been removed, while the effect of moisture is highly significant for wet concrete specimens with $RH > 70\%$. Consequently, for AASC it is reasonable and practical not to consider a correction factor to the air permeability, when the relative humidity at the surface region is below 65%.

This recommendation for the AASC air permeability measurement is consistent with the NC.

In addition, the air permeability of both AASC and NC falls as the compressive strength grades rise. The API values of AASC showed similar general trends as sorptivity for a given compressive strength grade but to different degrees. These observations clearly indicate that even with similar capillary porosity (as illustrated in **Figure 5**) and compressive strength (as given in **Table 2**), concrete specimens do not necessarily exhibit similar permeation properties (shown in **Figure 6** and **9**) and the concrete type could also significantly affect relevant performance. This is because the w/b of NC needed to be

lowered by a greater proportion to achieve the designed compressive strength. Thus, the pore structure of NC was improved that probably exceeded the benefits from hydration products from AASC. As such, the performance difference between NC and AASC cannot be judged by compressive strength alone.

4. Conclusion

From the experimental results represented in this study, the following conclusions can be drawn:

- 1) AASC has a rapid moisture loss rate up to 10 days of drying, afterwards the moisture at 20 mm in AASC becomes stabilised. Unlike NC, the strength grade (or w/b) of AASCs has no influence on changes in RH values at 20 mm irrespective of the drying duration. In this process, the RH values of AASC are always above 40 %, indicating that this drying regime is mainly to remove capillary moisture and hence, it can be used as a preconditioning regime for durability tests (such as air permeability, sorptivity) of AASC samples.
- 2) For a given compressive grade, AASC has a similar capillary porosity as NC, but more permeable in terms of air permeability and sorptivity. The air permeability of AASC increased with an increase in the drying duration, but became stable after 10 days of drying. Therefore, to eliminate the influence of moisture on air permeability and sorptivity, the AASC samples can be dried for 10 days at 40 °C or an RH value of <65% on the surface and at 20 mm is achieved.
- 3) Microstructure examination using moisture loss under different temperatures, SEM and MIP reveals that for a given compressive grade the AASC tends to have a higher porosity and more importantly, the pore size distribution of AASC is more continuous, which has a major effect on the permeation properties. In order to clearly explain the transport behaviours of AASC, measurement of pore structure in terms of size and numbers is more significant than in terms of volumes.

- 4) The results highlight the need to fully assess the durability performance of AASC. As expected, the compressive strength alone was not sufficient to justify the difference in durability behaviour between NC and AASC.

The pore structure of AASC is dependent on many factors, including the ingredients, mix design, curing conditions, and in an effort to produce durable AASC structures, in addition to specifying target compressive strength and maximum w/b ratio, it is essential to prescribe permeation properties which satisfy pre-specified requirements.

Acknowledgment

The experiments described in this paper were carried out in the concrete laboratory of Chongqing University and the authors acknowledge Chongqing University for providing facilities for the investigation reported in this paper. The authors thank financial supports provided by National Natural Science Foundation of China (Project NO. 51408078) and the Fundamental Research Funds for the Central University (Project NO. CDJXY130012). The supports from Queen's University Belfast, Ulster University and University of Leeds are highly appreciated.

Reference

- [1] J.K. Angell, J. Korshover, Estimate of the Global Change in Tropospheric Temperature Between 1958 and 1973, *Monthly Weather Review*, 103 (1975) 1007-1012.
- [2] D. Xu, Y. Cui, H. Li, K. Yang, W. Xu, Y. Chen, On the future of Chinese cement industry, *Cement and Concrete Research*, 78 (2015) 2-13.
- [3] E. Deir, B.S. Gebregziabiher, S. Peethamparan, Influence of starting material on the early age hydration kinetics, microstructure and composition of binding gel in alkali activated binder systems, *Cement and Concrete Composites*, 48 (2014) 108-117.
- [4] F. Pacheco-Torgal, Z. Abdollahnejad, A.F. Camoes, M. Jamshidi, Y. Ding, Durability of alkali-activated binders: A clear advantage over Portland cement or an unproven issue?, *Construction and Building Materials*, 30 (2012) 400-405.
- [5] I. Ismail, S.A. Bernal, J.L. Provis, R. San Nicolas, S. Hamdan, J.S.J. van Deventer, Modification of phase evolution in alkali-activated blast furnace slag by the incorporation of fly ash, *Cement and Concrete Composites*, 45 (2014) 125-135.
- [6] A. Wardhono, D.W. Law, T.C.K. Molyneaux, Long term performance of alkali activated slag concrete, *Journal of Advanced Concrete Technology*, 13 (2015), 187-192.
- [7] R.J. Thomas, S. Peethamparan, Alkali-activated concrete: Engineering properties and stress-strain behaviour, *Construction and Building Materials*, 93 (2015), 49-56.

- [8] S.A. Bernal, J.L. Provis, R.M. de Gutierrez, J.S.J. van Deventer, Accelerated carbonation testing of alkali-activated slag concrete/metakaolin blended concretes: Effect of exposure conditions, *Materials and Structures*, 48 (2015) , 653-669.
- [9] F. Collins, J.G. Sanjayan, Microcracking and strength development of alkali activated slag concrete, *Cem. Concr. Compos.*, 23 (2001) 345-352.
- [10] S.A. Bernal, J.L. Provis, D.J. Green, Durability of Alkali-Activated Materials: Progress and Perspectives, *Journal of the American Ceramic Society*, 97 (2014) 997-1008.
- [11] L.J. Parrott, Moisture conditioning and transport properties of concrete test specimens, *Materials and Structures*, 27 (1994) 460-468.
- [12] R.D. Hooton, S. Mindess, J.C. Roumain, A.J. Boyd, K. Rear, Proportioning and testing concrete for durability, *Concrete International*, 28 (2006) 38-41.
- [13] R.K. Dhir, P.C. Hewlett, Y.N. Chan, Near-surface characteristics of concrete prediction of carbonation resistance, *Magazine of Concrete Research*, 41 (1989) 137-143.
- [14] R.K. Dhir, P.C. Hewlett, Y.N. Chan, Near surface characteristics of concrete intrinsic permeability, *Magazine of Concrete Research*, 41 (1989) 87-97.
- [15] C. Andrade, M. Castellote, C. Alonso, C. Gonzalez, Non-steady-state chloride diffusion coefficients obtained from migration and natural diffusion tests. Part I-Comparison between several methods of calculation, *Materials and Structures*, 33 (2000) 21-28.
- [16] F.D. Lydon, D.K. Broadley, Effect of coarse aggregate on relative permeability of concrete, *Construction and Building Materials*, 8 (1994) 185-189.
- [17] H.M. Jennings, J.W. Bullard, J.J. Thomas, J.E. Andrade, J.J. Chen, G.W. Scherer, Characterization and modeling of pores and surfaces in cement paste: Correlations to processing and properties, *Journal of Advanced Concrete Technology*, 6 (2008) 5-29.
- [18] P.A. Claisse, Transport Properties of Concrete, *Concrete International*, 27 (2005) 43-48.
- [19] M.A. Wilson, M.A. Carter, C. Hall, W.D. Hoff, C. Ince, S.D. Savage, B. McKay, I.M. Betts, Dating fired-clay ceramics using long-term power law rehydroxylation kinetics, *Proceedings of the Royal Society A: Mathematical, Physical and Engineering Sciences*, 465 (2009) 2407-2415.
- [20] P.A.M. Basheer, Permeation analysis, in: R. V.S., J.J. Beaudoin (Eds.) *Handbook of Analytical Techniques in Concrete Science and Technology: Principles, Techniques and Applications*, Noyes Publications 2001, 658-727.
- [21] C. Galle, Effect of drying on cement-based materials pore structure as identified by mercury intrusion porosimetry, *Cement and Concrete Research*, 31 (2001) 1467-1477.
- [22] I. Maruyama, Y. Nishioka, G. Igarashi, K. Matsui, Microstructural and bulk property changes in hardened cement paste during the first drying process, *Cement and Concrete Research*, 58 (2014) 20-34.
- [23] H.F. Taylor, *Cement chemistry*, Thomas Telford, 1997.
- [24] S. Diamond, The microstructure of cement paste and concrete-a visual primer, *Cement and Concrete Composites*, 26 (2004) 919-933.
- [25] P.K. Mehta, P.J.M. Monteiro, *Concrete: Microstructure, Properties, and Materials*, 3rd ed., McGraw-Hill Professional, 2005.
- [26] F. Collins, J.G. Sanjayan, Cracking tendency of alkali-activated slag concrete subjected to restrained shrinkage, *Cement and Concrete Composites*, 30 (2000) 791-798.
- [27] I. Ismail, S.A. Bernal, J.L. Provis, S. Hamdan, J.S.J. van Deventer, Drying-induced changes in the structure of alkali-activated pastes, *Journal of Materials Science*, 48 (2013) 3566-3577.
- [28] M.M. Hossain, M.R. Karim, M.K. Hossain, M.N. Islam, M.F.M. Zain, Durability of mortar and concrete containing alkali-activated binder with pozzolans: A review, *Construction and Building Materials*, 93 (2015) 95-109.
- [29] K. Yang, P.A.M. Basheer, Y. Bai, B.J. Magee, A.E. Long, Development of a new in situ test method to measure the air permeability of high performance concretes, *NDT & E International*, 64 (2014) 30-40.

- [30] M. Romer, Effect of moisture and concrete composition on the Torrent permeability measurement, *Materials and Structures*, 38 (2005) 541-547.
- [31] K. Chen, C.H. Yang, Q. Pan, S. Zhao, Z.D. Yue, Drying shrinkage characteristics of alkali-slag cement mortar, *Journal of Chongqing University(Natural Science Edition)*, 35 (2012) 64-68.
- [32] K. Yang, P.A.M. Basheer, Y. Bai, B.J. Magee, A.E. Long, Assessment of the effectiveness of the guard ring in obtaining a uni-directional flow in an in situ water permeability test, *Materials and Structures*, 48 (2015) 167-183.
- [33] X.C. Pu, C.H. Yang, C.C. Gan, Investigation of setting time of high strength alkali-activated slag cement and concrete, *Cement*, 10 (1992) 32-36.
- [34] GB-175, Common Portland cement, Standardization Administration of the People's Republic of China, SAC, Beijing, 2007, Page 16.
- [35] GB/T-14684, Sand for construction, Standardization Administration of the People's Republic of China, SAC, Beijing, 2011, Page 28.
- [36] GB/T-14685, Pebble and crushed stone for construction, Standardization Administration of the People's Republic of China, SAC, Beijing, 2011, Page 1-30.
- [37] BS:1881-125, Methods for mixing and sampling fresh concrete in the laboratory, BSI, London, 1986, Page 1-10.
- [38] GB/T-50080, Standard for test method of performance on ordinary fresh concrete, Standardization Administration of the People's Republic of China, SAC, Beijing, 2002, Page 1-31.
- [39] BS-EN:13057, Products and systems for the protection and repair of concrete structures-Test methods: Determination of resistance of capillary absorption, BSI, London, 2002, pp. 1-16.
- [40] L.J. Parrott, Influence of cement type and curing on the drying and air permeability of cover concrete, *Magazine of Concrete Research*, 47 (1995) 103-111.
- [41] C. Shi, Strength, pore structure and permeability of alkali-activated slag mortars, *Cement and Concrete Research*, 26 (1996) 1789-1799.
- [42] P. Steins, A. Poulesquen, O. Diat, F. Frizon, Structural Evolution during geopolymerization from an early age to consolidated material, *Langmuir*, 28 (2012) 8502-8510.
- [43] W. Chen, H.J.H. Brouwers, The hydration of slag, Part 1: reaction models for alkali-activated slag, *Journal of Materials Science*, 42 (2007) 428-443.
- [44] C. Frank, S. J.G., Effect of pore size distribution on drying shrinkage of alkali-activated slag concrete, *Cement and Concrete Research*, 30 (2000) 1401-1406.
- [45] S. Al-Otaibi, Durability of concrete incorporating GGBS activated by water glass, *Construction and Building Materials*, 22 (2008) 2059-2067.
- [46] M.R. Karim, M.M. Hossain, M.N.N. Khan, M.F.M. Zain, M. Jamil, F.C. Lai, On the utilisation of pozzolanic wastes as an alternative resource of cement, *Materials*, 7 (2014) 7809-7827.
- [47] C. Ince, M.A. Carter, M.A. Wilson, A. El-Turki, R.J. Ball, G.C. Allen, N.C. Collier, Analysis of the abstraction of water from freshly mixed jointing mortars in masonry construction, *Materials and Structures*, 43 (2009) 985-992.
- [48] S.A. Bernal, R. Mejia de Gutierrez, A.L. Pedraza, J.L. Provis, E.D. Rodriguez, S. Delvasto, Effect of binder content on the performance of alkali-activated slag concretes, *Cement and Concrete Research*, 41 (2011) 1-8.
- [49] F.U.A. Shaikh, Effects of alkali solutions on corrosion durability of geopolymer concrete, *Advances in Concrete Construction*, 2 (2014) 109-123.
- [50] K. Yang, P.A.M. Basheer, B.J. Magee, Y. Bai, Investigation of moisture condition and Autoclam sensitivity on air permeability measurements for both normal concrete and high performance concrete, *Construction and Building Materials*, 48 (2013) 306-314.

List of Table

Table 1 Experimental programme

Table 2 Mix proportions and general properties of concrete tested in this study

Table 3 Chemical composition of GBFS and PC (percent by mass, %)

List of Figure

Figure 1 Illustration for incremental immersion procedure

Figure 2 The probe of measuring RH at surface and in the drilled cavities

Figure 3 Illustration of surface air permeability test apparatus

Figure 4 Relative humidity results at surface and in the drilled cavities after drying (40 °C, RH 35%) for different periods

Figure 5 Porosity of AASC and NC for a given compressive grade

Figure 6 Sorptivity of AASC and NC for a given compressive grade

Figure 7 Comparison of SEM results for AASC and NC for a given compressive strength grade

Figure 8 Pore size distribution of AASC and NC determined by MIP measurements

Figure 9 Influence of drying duration on air permeability of AASC and NC

Figure 10 Relationship between normalised air permeability index and relative humidity in the 20mm hole

Table 1 Experimental programme

Variable		Level and parameter investigated
Concrete	Type	AASC, normal concrete (NC)
	Compressive strength grade	C30, C45, C60
Moisture condition	Oven dry at 40 °C for 5, 10, 15, 20, 25 day	Relative humidity (RH) measurements on surface and in 20 mm cavity
Properties measured	Permeation properties	Air permeability, sorptivity
	General properties	Air content, slump, porosity, compressive strength

Table 2 Mix proportions and general properties of concrete tested in this study

Concrete type	AASC			NC		
	C30	C45	C60	C30	C45	C60
Strength grade	C30	C45	C60	C30	C45	C60
Binder (GBFS for AASC and Portland cement for NC) (kg/m ³)	400	400	400	380	420	480
Water (kg/m ³)	157.6	137.6	117.6	235	165	165
Superplasticiser (%)	-	-	-	0.5	0.8	1.5
Water glass, Ms: 1.2 (kg/m ³)	82.5	82.5	82.5	-	-	-
NaOH (kg/m ³)	12.9	12.9	12.9	-	-	-
Fine aggregate (kg/m ³)	740	785	790	725	785	765
Coarse aggregate (kg/m ³)	1110	1085	1065	1035	1100	1050
Slump (mm)	200	180	145	165	180	195
Air content (%)	1.8	2.1	1.6	1.5	1.7	1.8
Compressive strength at 28 day (MPa)	34.6	53.6	66.7	36.8	55.1	69.5

Note:

1. The Na₂O dosage was kept constant, 5% of the binder content;
2. Superplasticiser was used for NC.
3. Superplasticiser refers to percentage of cement content.
4. Ms is defined as the mass ratio of SiO₂ to Na₂O.

Table 3 Chemical composition of GBFS and PC (percent by mass, %)

composition	SiO ₂	Al ₂ O ₃	Fe ₂ O ₃	MgO	CaO	Na ₂ O	K ₂ O	Loss	Other
GBFS	31.63	13.42	1.32	9.12	36.35	0.34	0.46	0.61	6.75
PC	21.33	5.80	2.57	2.41	60.21	0.70	0.21	-	6.67

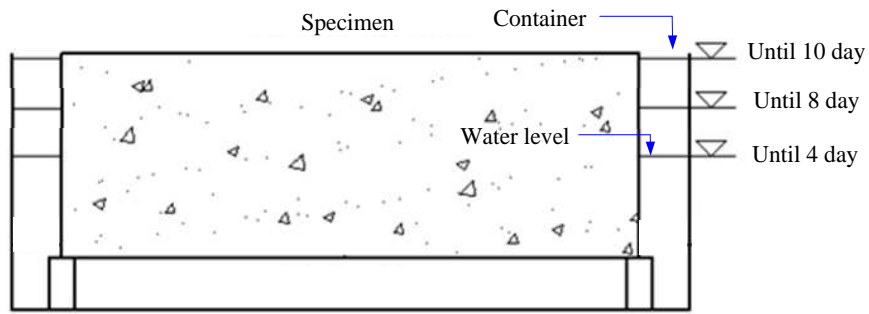


Figure 1 Illustration for incremental immersion procedure



Figure 2 The probe of measuring RH at surface and in the drilled cavities

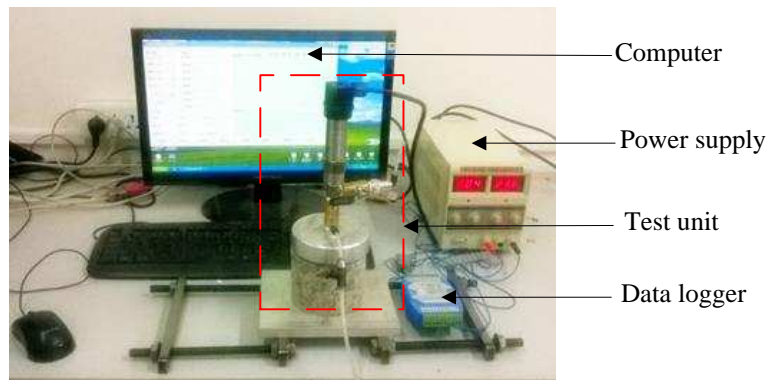


Figure 3 Illustration of surface air permeability test apparatus

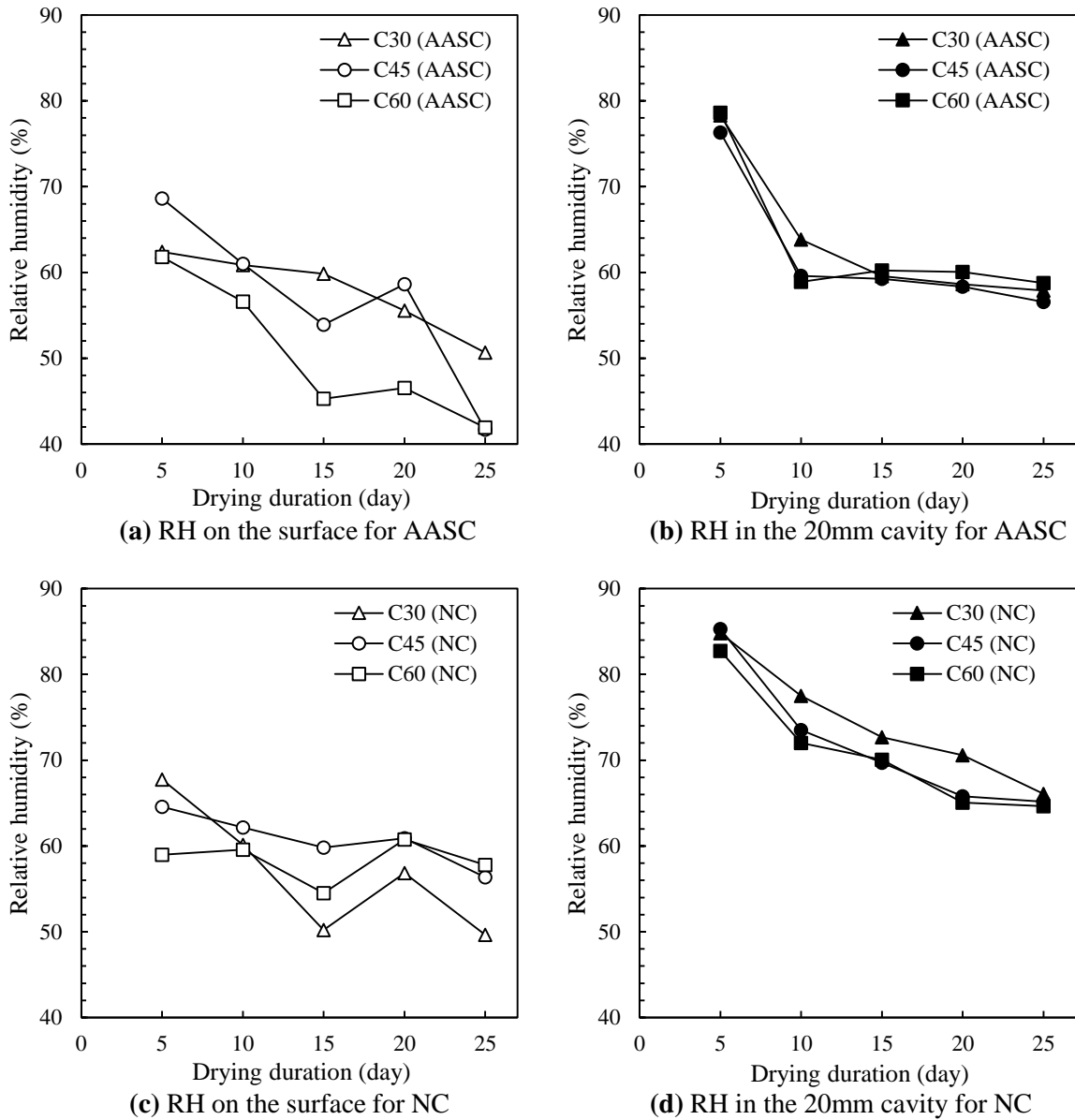


Figure 4 Relative humidity results at surface and in the drilled cavities after drying (40 °C, RH 35%) for different periods

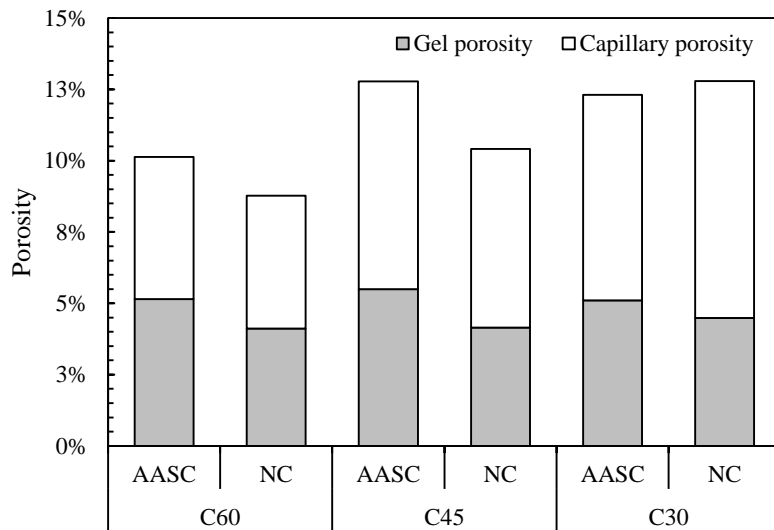


Figure 5 Porosity of AASC and NC for a given compressive grade

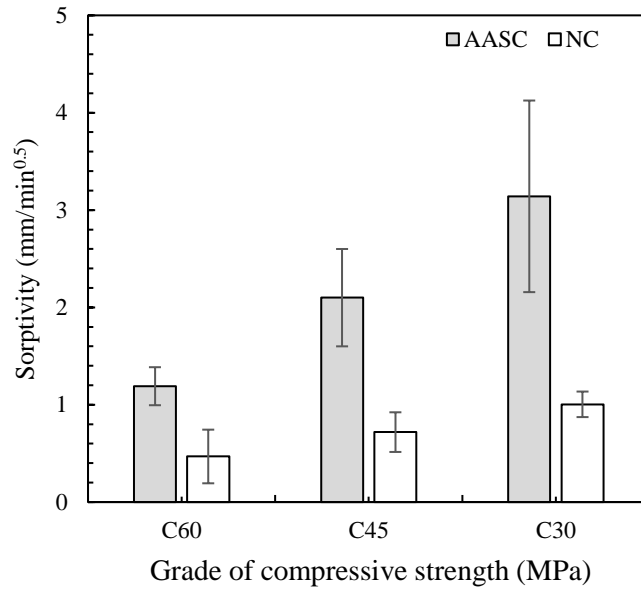


Figure 6 Sorptivity of AASC and NC for a given compressive grade

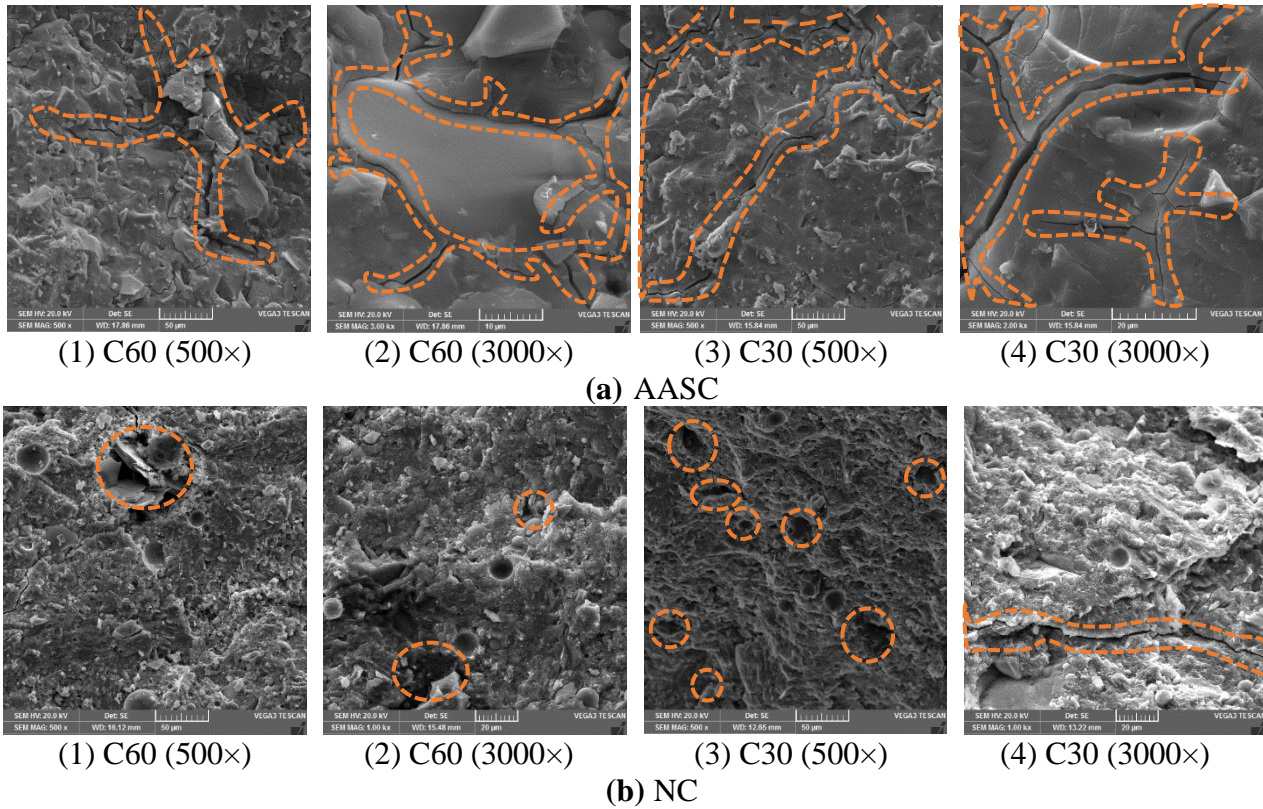
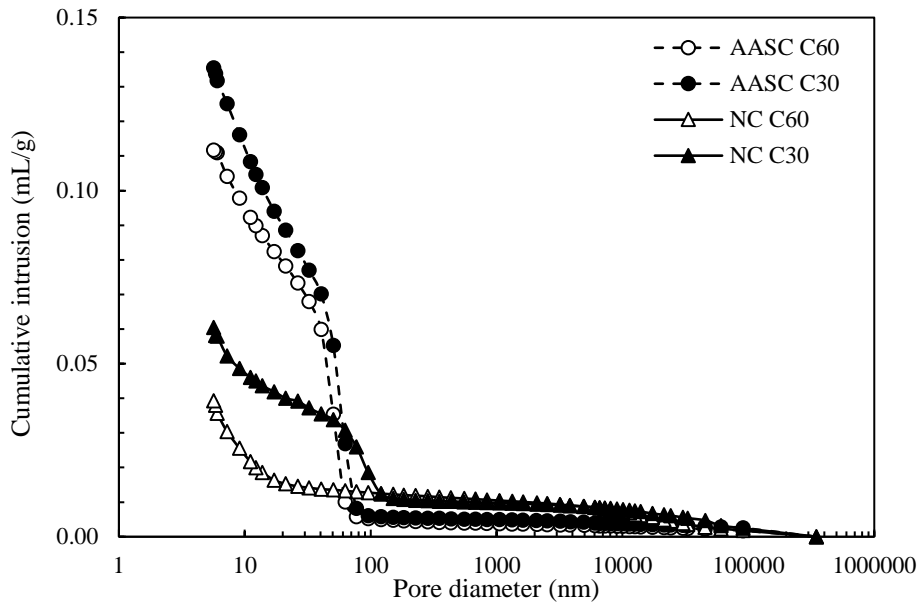
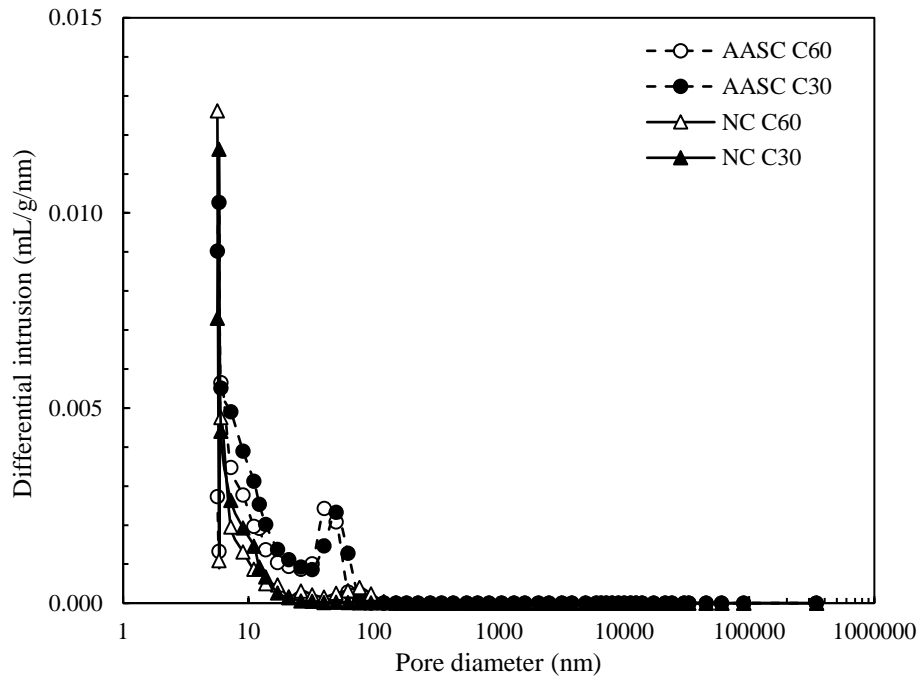


Figure 7 Comparison of SEM results for AASC and NC for a given compressive strength grade



(a) Cumulative intrusion Vs Pore diameter



(b) Differential intrusion Vs Pore diameter

Figure 8 Pore size distribution of AASC and NC determined by MIP measurements

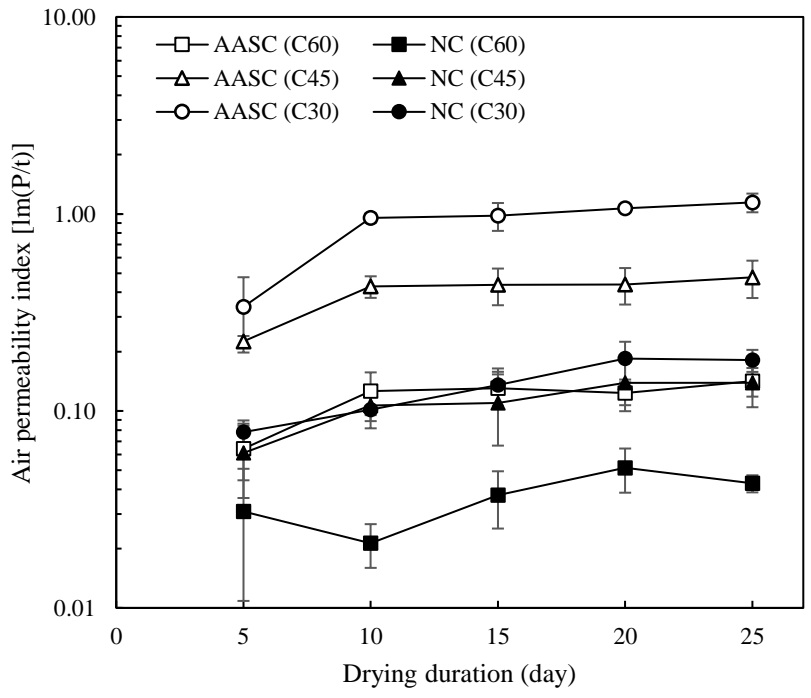


Figure 9 Influence of drying duration on air permeability of AASC and NC

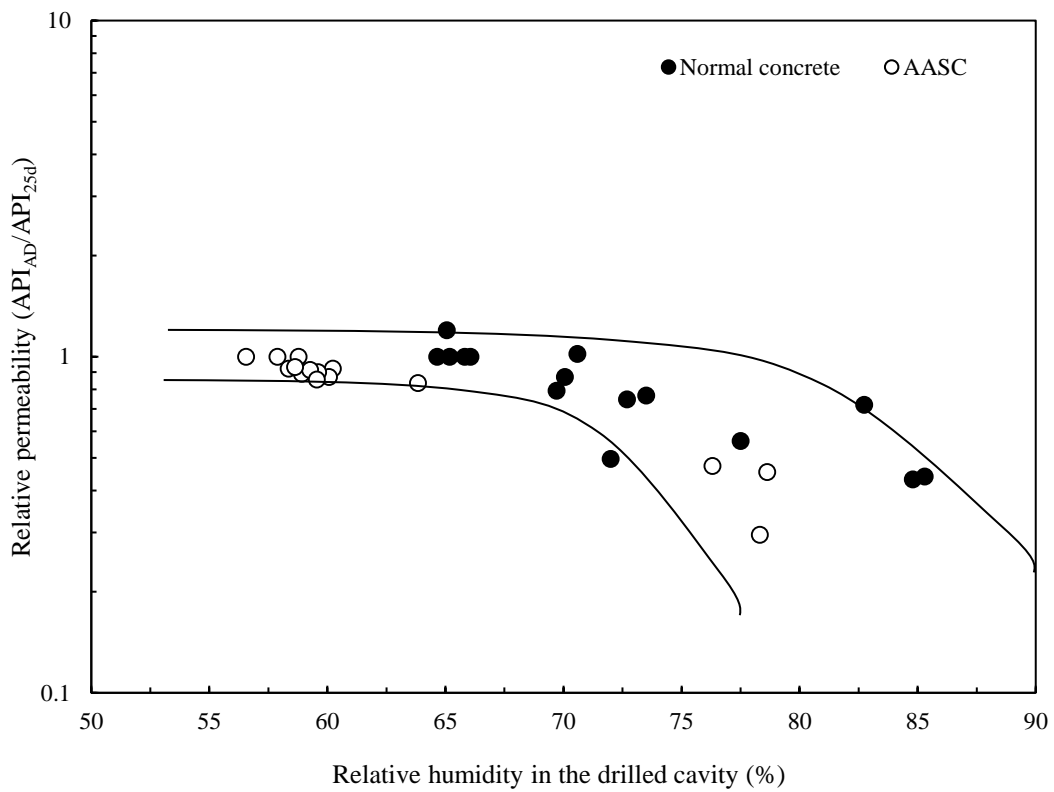


Figure 10 Relationship between relative air permeability index and relative humidity in the 20 mm cavities